Type of contribution: Regular Paper
Number of text pages: 23
Number of tables: 0
Number of figures: 4
Supplementary files: 1

Turnover of bacterial biomass to soil organic matter via fungal biomass and its metabolic implications

Tiantian Zheng[1,2], Anja Miltner[2], Chao Liang[1,2*], Karolina M. Nowak[2,3], Matthias Kästner[2]

1. Key Laboratory of Forest Ecology and Management, Institute of Applied Ecology, Chinese Academy of Sciences, Shenyang 110016, China
2. UFZ-Helmholtz Centre for Environmental Research, Department of Environmental Biotechnology, Permoserstr. 15, 04318 Leipzig, Germany
3. Chair of Geobiotechnology, Technische Universität Berlin, Ackerstraße 76, 13355 Berlin, Germany

Highlights

- Amino sugars are more stable biomarkers than amino acids in proteins.
- Bacterial biomass residue-derived C is stabilized via fungal residues.
- A succession of different pathways in central metabolism was observed.
- Bacterial biomass C is partially preserved over the time of incubation.

Abstract

Microbial biomass residues play a significant role in biogeochemical cycling but the mechanism by which material from microbial sources is sequestered in soil organic matter still remains elusive. Although we previously investigated the detailed turnover process of Gram-negative bacterial biomass (*E. coli*) derived carbon (C) in soil and found indications that fungi were the first clade to incorporate *E. coli*-derived C, no reliable estimate is available for the amount of bacterial biomass-derived C that is stabilized via fungal residues during turnover in soils. Here we tracked ^{13}C-amino sugars (from chitin and peptidoglycan) and amino acids (from proteins) in order to shed light onto the bacterial and fungal food web. During incubation, ^{13}C-amino acids decreased significantly, whereas ^{13}C-amino sugars changed only slightly over time, suggesting that amino sugars as biomarkers are relatively stable compared to amino acids. The ratio of ^{13}C-fungal derived glucosamine to ^{13}C-muramic acid significantly increased before day 14, then levelled off until the end of the experiment. This further highlighted that bacterial C was stabilized in soil by conversion to fungal biomass grown on the bacterial biomass. Interestingly, the shifts in ^{13}C-amino acids distribution pattern reflect three phases of the central metabolism: in the beginning, the added biomass was low in carbohydrates compared to the needs of the active microbes, resulting in a dominance of the glyoxylate cycle. In a second phase, the general metabolism and thus the tricarboxylic acid cycle (TCA) was very active, most probably supported by the use of a mixture of compounds from soil organic matter. This phase also included anaplerotic reactions resulting in C incorporation from CO_2. Finally, metabolism slowed down and thus the TCA cycle was less active and C rather than energy was preserved. In summary, our study provided evidence that bacterial biomass residues were predominantly utilized by fungi; thus, at the end, the C was mainly stabilized as fungal necromass. Our results also indicated that bacterial biomass residues are turned over for preservation of C (~50%) rather than energy towards the end of the incubation. This may thus be an important pathway for soil organic carbon sequestration in soil.

Keywords: Amino sugars; Microbial necromass; Amino acids; TCA cycle; Soil organic

matter

1. Introduction

Studies of the sequestration of soil organic carbon (SOC) have dramatically increased in recent years as soil organic matter (SOM) is an important natural resource which supports the provision of food, helps in regenerating fertility, and is essential for many vital ecosystem services, such as nutrient transformations, water storage, and habitat for biodiversity (Carter et al., 2002; Chazdon et al., 2009; Smith et al., 2015). The important role of soil microorganisms as catalysts for SOM formation has long been recognised (Kögel-Knabner, 2002). Importantly, soil microorganisms do not only promote plant litter and SOM transformation and turnover, but also contribute with their biomass residues: the contribution of microbial necromass has been estimated to range from 30 to 61.8% (Liang et al., 2019). Such high contributions of microbial necromass to SOM have important implications for understanding SOM transformation and sequestration processes. In particular, microbial necromass, and its turnover and stabilization, have been considered to be of great significance for SOM formation (Miltner et al., 2012; Hu et al., 2020). Therefore, understanding the detailed processes of microbial biomass residues carbon (C) transformation is essential for improving our understanding of the mechanism of SOM formation.

Some earlier studies investigated the turnover of microbial residues by means of mass-balance experiments with labelled microorganisms of various classes. These studies showed that between 34 and 66% of the initial microbial biomass C remains in soil, whereby less than 15% of the label is present in other living microbial biomass; thus around 20-50% of the label from the various classes of microorganisms remains in non-living SOM in these experiments (Kindler et al., 2006; Miltner et al., 2012; Schweigert et al., 2015; Zheng et al., 2021), confirming that microbial biomass residues C contributes significantly to the formation of SOM. Going even further, Zheng et al. (2021) followed the detailed ^{13}C cycling through the microbial food web during the turnover process and found indications that fungi were the pioneer clade to utilize C derived from the Gram-negative bacterial residues. This may be crucial for the potential contribution of the ^{13}C in bacterial biomass residues to SOM, as the turnover times of fungal material have been reported to be much longer than those of bacterial residues due to the different compositions of fungal and bacterial cell walls (Feofilova, 2010;

Schweigert et al., 2015; Fernandez et al., 2016). However, at present no reliable assessment is available for how much of the bacterial biomass residue-derived C is stabilized via fungal residues during turnover in soils. This, however, would be an essential piece of information for potential controls on SOM stabilization. Amino sugars are microbial cell wall components that persist in soils after cell death and can reflect the microbial residue dynamics (Amelung, 2001; Joergensen, 2018). Three amino sugars [glucosamine (GluN), galactosamine (GalN) and muramic acid (MurA)] are commonly used to evaluate the accumulation of microbially derived C in soil (Amelung, 2001; Joergensen, 2018). In addition, the ratio GluN/MurA reflects the relative accumulation of fungal vs. bacterial-derived residues in soils (Amelung, 2001; van Groenigen et al., 2010), based on their different cell wall compositions. Fungal cell walls contain chitin, which is a polymer of GluN, while a main constituent of bacterial cell walls is murein, which contains both GluN and MurA at a ratio of 2:1 (Engelking et al., 2007; Joergensen, 2018; Liu et al., 2019). Therefore, amino sugar analysis during bacterial biomass residues turnover can provide estimates not only for the amount of microbial residues in SOM, but also for the ratio of fungal to bacterial-derived residues. GalN is of mixed fungal and bacterial origin, thus is useful overall quantification of biomass residues, but in contrast to the GluN and MurA it is not specific for sources (Joergensen, 2018). As the turnover rates of the different types of necromass differ (see above), this is an important knowledge which could help in estimating how stable the SOM formed from the residues is in soil.

Proteins, which consist of amino acid chains, are the most abundant components of bacterial cells. Proteinaceous amino acids are tightly associated with soil fertility and primary production (Chapin et al., 2011) because they are important C and nutrient sources in soils (Stevenson, 1982). They were also recognized for their important role in the stabilization and destabilization of SOC and N (Rillig et al., 2007; Jones and Kielland, 2012; Farrell et al., 2014). Amino sugars and amino acids hydrolysed from peptidoglyan/chitin or proteins, respectively, are particularly useful microbial biomarkers because their polymers are relatively stable against degradation, and are preserved in soils for long times after cell death (Amelung et al., 2001). A study which quantified the decomposition of proteins and microbial cell walls showed that the turnover times of microbial cell wall material and soil protein are comparable across various ecosystems (Hu et al., 2020). However, we are currently lacking knowledge about how stable amino sugars or bacterial-derived amino acids are during the

decomposition process. This lack of information on the stability of these frequently used biomarkers largely limits our understanding of soil C and N cycling as well as the microbial contribution of the major groups of microorganisms to SOM formation. Microbes can assimilate amino acids by enzymatically depolymerizing proteins, and use them as substrates or building blocks for growth; however, amino acids are also *de novo* biosynthesized by the microbes during growth and biomass production (Price et al., 2018; Kästner et al., 2021). This is also the case during organic matter degradation (Amelung et al., 2001; Hobara et al., 2014). As a result, the transformation dynamics of soil amino acids are tightly associated with microbial proliferation (Hu et al., 2016). The use of ^{13}C-labelled bacterial biomass residues and isotopic analysis of biomarker amino acids can thus provide information about the turnover of total proteinaceous amino acids. Specifically, the observations of transformation dynamics of individual amino acids can provide deeper insights about how the bacterial-derived C is allocated between different pathways of the central metabolism and distributed over the microbial food web based on tricarboxylic acid cycle (TCA) analysis (Nowak et al., 2018). The TCA is a central catabolic biochemical pathway providing ATP and reduction equivalents. However, certain metabolites from this cycle are also used for synthesis of particular amino acids. TCA cycle analysis is therefore a powerful tool for obtaining information about the detailed metabolic processes and pathways of bacterial necromass contribution to SOM formation (Feisthauer et al., 2008; Miltner et al., 2005a; Miltner et al., 2005b). This contribution has been reported to be important (Miltner et al., 2009), but mechanisms are unknown.

Therefore, in our study, we determined the fate of the ^{13}C-labelled bacterial biomass residues by analysis of the label in amino sugars. We also traced the incorporation of the bacterial residue-derived ^{13}C into proteins by analysis of the concentrations and isotopic signatures of the amino acids. The objectives of this study were: (1) quantifying the relative contributions of fungal-derived C and bacterial-derived C residues to SOM formation together with the changes over time during the turnover process of *E. coli* derived C, (2) assessing whether and how amino sugars or amino acids are stable biomarkers in soil, and (3) tracing the detailed metabolic pathway of C from microbial biomass residues to stabilized SOM over time.

2. Materials and Methods

2.1 Soil, strain and experimental setup

Soil was incubated with ^{13}C-labelled cells of the Gram-negative bacterial strain *E. coli* K12; details of the experiments were described previously (Zheng et al., 2021). The soil material was from the agricultural long-term experiment "Statischer Düngungversuch" located in Bad Lauchstädt, Germany. The plot was cultivated with crop rotation (sugar beet, summer barley, potatoes and winter wheat) and fertilized with farmyard manure (30 t ha^{-1} y^{-1}). The soil material has been characterised previously (Zheng et al., 2021) and by new analyses. It was a silty loam (210 g kg^{-1} clay, 680 g kg^{-1} silt, 110 g kg^{-1} sand) with a TOC content of 26.3 g kg^{-1}, a total nitrogen content of 2.8 g kg^{-1}, a pH of 6.6, and a maximum water holding capacity of 375 g kg^{-1}. The natural abundance in ^{13}C of the soil was 1.077 at% ^{13}C. The soil was stored at 4 °C and passed through a 2-mm sieve before use. The soil was adjusted to 40% of water holding capacity and pre-incubated at 20 °C for 10 days before the incubation experiment.

As a model for Gram-negative bacterial biomass residues, we used the strain *E. coli* K12 in this incubation experiment. ^{13}C-labelled bacterial biomass was produced by culturing *E. coli* in an optimized mineral medium with 4 g l^{-1} ^{13}C-labelled glucose (D-glucose-U-$^{13}C_6$, 99 at% ^{13}C; Cambridge Isotope Laboratories, Andower, USA) as the sole carbon and energy source, as described by Zheng et al. (2021). We amended the soil with 2.0×10^8 ^{13}C-labelled *E. coli* cells per gram of soil (dw), corresponding to 36 µg ^{13}C g^{-1} soil (initial amount added) for the incubation experiment. The enrichment of the labelled microbial biomass was > 90 at% ^{13}C. In addition, the same soil amended with the same number of unlabelled *E. coli* cells, as well as unamended soil, were included in the experiment as unlabelled and unamended controls, respectively. The preparation of the soil for the incubation experiments took totally around 3 to 4 hours after adding the *E. coli* cells. The control treatments were prepared and incubated under the same conditions, and they served to account for the natural abundance of ^{13}C in the soil, in the amino sugars and in the amino acids. The water content of the soil mixture was finally adjusted with soil leachate to 60% of the maximum water holding capacity. We sampled and analysed the soil on days 0, 7, 14, 30, 60 and 120 from the start of the experiment. The detailed experimental setup was described by Zheng et al. (2021).

2.2 Quantification of amino sugars and their isotope compositions.

Amino sugars were extracted and analysed according to Zhang and Amelung (1996). In brief, we weighed soil samples (around containing ± 0.4 mg N) and hydrolysed them with 10 mL 6 M HCl at 105 °C for 8 h to obtain amino sugar monomers from the

polymers chitin and peptidoglycan. After cooling the flasks to room temperature, 100 μL of the internal standard inositol (1mg/mL in water) was added to each flask and mixed in by swirling. After subsequently filtering the solution, the filtrate was dried in a rotary evaporator, and the dried residue was resuspended in 10 ml water. The pH value was adjusted to 6.6-6.8 and then the samples were centrifuged and lyophilized. Amino sugars were extracted from the lyophilized residues with methanol and derivatized. Their concentration was quantified using GC/MS, and their isotopic composition was determined by means of GC/IRMS. Details of amino sugar analytical conditions are presented in supplementary material I "GC/MS and GC/IRMS settings for quantitative, qualitative and isotopic composition analyses of amino sugars".

The $\delta^{13}C$ values of soil amino sugars were calculated according to the equation:

$$\delta^{13}C_{As} = \frac{(No._{Der} \times \delta^{13}C_{Der} - No._{Acet} \times \delta^{13}C_{Acet})}{No._{As}}$$

where No. $_{As}$ is the number of C atoms in the amino sugar molecule (No. $_{As}$ = 6), No. $_{Acet}$ is the number of C atoms in the acetyl group used for derivatization (No. $_{Acet}$ = 10) and No. $_{Der}$ is the number of C atoms in the amino sugar derivatives (No. $_{Der}$ = 16). The $\delta^{13}C$ of the carbon atoms used for derivatization ($\delta^{13}C_{Acet}$) was estimated separately using amino sugar standards (Glaser and Gross, 2005).

The stable C isotope ratios in the various C pools were expressed as at% ^{13}C, which was converted from $\delta^{13}C$, a value relative to the Pee Dee Belemnite standard, as follows:

$$at\%^{13}C = \frac{100 \times 0.01118 \times (\frac{\delta^{13}C}{1000} + 1)}{1 + 0.01118 \times (\frac{\delta^{13}C}{1000} + 1)}$$

As an index for fungal residues, we calculated fungal-derived GluN (F-GluN) by subtracting bacterial GluN from total GluN, assuming that GluN and MurN occur at 2:1 molar ratio in bacterial cells (Engelking et al., 2007). The following equation was used (Shao et al., 2017):

$$F - GluN = (GluN/179.2 - 2 * MurA/251) * 179$$

Mannosamine is not specific for any biomass source and usually occurs at low concentration with strong variation; therefore, it is often not presented in recent studies (Joergensen et al., 2018; Yang et al., 2022).

2.3 Quantification of amino acids and their isotope compositions.

Amino acids were hydrolysed from proteins. The detailed extraction, purification and derivatization methods for amino acid was described in previous studies (Nowak et

al., 2013, 2018). In short, the proteins were hydrolysed to amino acids at 110 °C for 22 h using 6 M HCl and the samples were purified over cation exchange resin (DOWEX 50W-X8; Nowak et al., 2011). The identity and quantity of amino acids were analysed by means of GC-MS (Agilent GC7890A, MS 5975C, Waldbronn, Germany); the isotopic compositions of the amino acids were determined by means of GC-C-IRMS (Finnigan MAT 253 coupled to a Trace GC, Thermo Electron, Bremen, Germany). The isotopic signatures of the amino acids were corrected for C introduced during derivatization according to (Silfer et al., 1991). Details on the analytical procedure and conditions for amino acids are presented in supplementary material I "GC/MS and GC/IRMS settings for quantitative, qualitative and isotopic composition analyses of amino acids".

2.4 Statistical analyses

All incubation experiments were prepared in triplicate. The results are shown as means; the error bars represent the standard error of the three replicates. Absolute abundance and percentage of ^{13}C-amino sugars and total amino sugars, ^{13}C-amino acids and total amino acids at different incubation times were tested for statistically significant differences between sampling times using one-way analysis of variance (ANOVA) and a Tukey HSD post-hoc test. Data analysis was conducted in the R statistical environment (version 3.0.3) (R Development Core Team, 2014).

3. Results

3.1 Abundance of total and bacterial-derived amino sugars

We found that the concentrations of total amino sugars were quite stable over time during the incubation (Fig. 1A). Neither the concentrations nor the percentage distribution of GluN, GalN, MurA changed significantly over time (Fig. 1A and 1B). The amino sugars were dominated by GluN (63% ± 0.4%), followed by GalN (32% ± 0.6%). MurA only contributed about 5.4 % ± 0.3% to the total amino sugars (Fig. 1B).

In contrast, there was no difference of ^{13}C in total amino sugars between day 0 (4.53 ± 0.15 nmol g^{-1}), day 7 (4.35 ± 0.18 nmol g^{-1}), day 14 (4.83 ± 0.17 nmol g^{-1}) and day 30 (4.55 ± 0.10 nmol g^{-1}), only at the end of the incubation, after 120 days, it decreased to 3.91 ± 0.11 nmol g^{-1} (Fig. 1C). Initially, the abundance of ^{13}C-GalN was very low (0.11 ± 0.03 nmol g^{-1}), but it increased during the 120 days of incubation to 0.72 ± 0.06 nmol g^{-1} (Fig. 1C). This mainly happened during the first 14 days and indicated substantial

turnover of the added ^{13}C-labelled bacterial biomass. The absolute amounts of the other two labelled amino sugars, ^{13}C-GluN and ^{13}C-MurA, decreased steadily to 80% and 36%, respectively, of their initial amounts over time (Fig. 1C). With respect to the relative contributions of the three amino sugars, we found a clear trend that the percentage of ^{13}C-GalN increased from about 3% to 21% over time at the expense of both ^{13}C- GluN and ^{13}C-MurA (Fig. 1D). Although ^{13}C-GluN and ^{13}C-MurA both decreased during incubation time (Fig. 1D), the ratio of ^{13}C-F-GluN to ^{13}C-MurA (^{13}C-F-GluN/^{13}C-MurA) increased from 4.39 to 10.76 during incubation (Fig. 2). Most of this increase happened during the first 7 days; in this period of time the ratio of ^{13}C-F-GluN/^{13}C-MurA increased to 8.71 ± 0.45 (Fig. 2), indicating that ^{13}C-MurA decreased faster than ^{13}C-F-GluN over time.

3.2 Abundance of total and bacteria-derived amino acids

During the 120 days incubation, the total amount of hydrolysable amino acids increased over time from 60 ± 3.19 μmol g^{-1} to 151 ± 3.60 μmol g^{-1} (Fig. 3A), indicating formation of amino acids during incubation. ^{13}C-amino acids contributed only about 1% to the total amino acids, and in contrast to the total amount of amino acids, ^{13}C-amino acids significantly decreased during incubation, from 1.9 ± 0.14 μmol g^{-1} to about 1 ± 0.04 μmol g^{-1} (Fig. 3A and Fig. 3B). The decrease was fast during the first 30 days of incubation, thereafter the amount of ^{13}C-amino acids remained fairly stable. In summary, about 54% of the initial *E. coli*-derived amino acids had been degraded at the end of the incubation experiment. The increase of total amino acid concentration with a concomitant decrease in the amount of ^{13}C-labelled amino acids indicates that the amino acids newly formed during incubation were mainly unlabelled; the C thus did not originate from the added ^{13}C biomass residues.

The pattern of ^{13}C distribution among the individual amino acids changed considerably over time (Fig. 3D). This allowed us to follow the fate of the C bound in bacterial biomass residues during metabolic cycling in detail. In particular, between day 0 and day 7, the relative share of ^{13}C in glycine increased from 5.9% to 15.0% and the share of ^{13}C in alanine increased from 16.4% to 25.8%. In contrast, the shares of leucine decreased from 13.2% to 8.0%, of isoleucine from 6.5% to 4.1% and of lysine from 11.3% to 8.1%. Seven days later, from day 7 to day 30, the label in the glutamate and aspartate increased. In brief, the percentage of *E. coli*-derived C bound in glutamate increased from 5.8% to 7.7%. For aspartate, the highest amounts of ^{13}C were found on day 30 (9.4%) compared to other incubation times, while the share of ^{13}C-isoleucine decreased

292 from 4.1% to 3.3%, of ^{13}C-lysine decreased from 8.1% to 6.5%, and of ^{13}C-alanine
293 decreased from 25.8% to 21.8% from day 7 to day 30. After 30 days of incubation, the
294 share of ^{13}C decreased from 7.7% to 5.8% in glutamate and from 9.4% to 5.9% in
295 aspartate, while the share of label detected in alanine increased from 21.8% to 29.0%
296 and in valine from 5.9% to 7.5% (Fig. 3D).
297

298 # 4. Discussion

299 In the study we presented the fate of the ^{13}C-label derived from a Gram-negative
300 bacterium in soil. In particular, based on the changes of the ^{13}C-F-GluN/^{13}C-MurA, we
301 could show that (1) ^{13}C-bacterial amino sugars decreased faster than ^{13}C-fungal amino
302 sugars during the incubation, (2) the pattern of amino acids as well as their ^{13}C
303 enrichment changed significantly, and (3) the pattern of the ^{13}C-amino acids changed,
304 which might be related with shifts in the metabolism of the labelled substrate (see below
305 for a detailed explanation) and a shift in the use of the substrate as a C or energy source
306 (Gunina and Kuzyakov, 2022).

307 ***4.1 Amino sugars as biomarkers are relatively stable compared to amino acids***

308 The concentrations of total amino sugars and the constant pattern of GluN, GalN
309 and MurA over time during the incubation (Fig. A and B) confirmed that amino sugars
310 are suitable as biomarkers for microbial necromass from the view of stabilization (Zhang
311 and Amelung, 1996). Also the amount of ^{13}C in total amino sugar was relatively stable
312 compared to ^{13}C in total amino acids: about 50% of the *E. coli*-derived amino acids were
313 degraded, whereas ^{13}C in total amino sugar decreased only slightly towards the end of
314 the incubation, again suggesting that amino sugars are more stable biomarkers than
315 amino acids (Fig. 1C and Fig. 3C). The reason for the higher stability of amino sugars
316 may be the different reactivities of the corresponding polymers towards hydrolysis.
317 Hydrolysis is the first step for degradation of protein or peptidoglycan polymers because
318 high molecular weight compounds cannot be transported into the cell for further
319 metabolism. Amino sugars occur mainly in peptidoglycan and chitin, which are
320 considered to be more difficult to hydrolyse than proteins, i.e. amino acid polymers
321 (Gunina et al., 2017). Proteins are thus considered to have a faster turnover than the
322 microbial cell wall components peptidoglycan or chitin.

323 ***4.2 Turnover of bacterial biomass to soil organic matter via fungal biomass***

324 The relative abundance of ^{13}C-GluN and ^{13}C-MurA both decreased during

incubation time (Fig. 1D). The abundance of ^{13}C-MurA decreased dramatically, obviously because the labelled *E. coli* added at the beginning of the incubation started to lyse and the peptidoglycan was degraded. As no other external substrates were added, the organisms could only grow on compounds mobilized from SOM and the bacterial residues added; the latter are generally decomposed relatively easily compared to fungal residues (Schweigert et al., 2015; Six et al., 2006). The ratio of ^{13}C-F-GluN/^{13}C-MurA can be used to assess the relative accumulation of fungal-versus bacterial-derived residues in soil (Amelung, 2001; Joergensen et al., 2018). Interestingly, we observed that the ratio of ^{13}C-F-GluN/^{13}C-MurA significantly increased during incubation until day 14. Although we cannot preclude bacterial reuse of ^{13}C-F-GluN and ^{13}C-MurA, the faster decrease of ^{13}C-MurA compared to ^{13}C-F-GluN until day 14 (Fig. 2) indicates that *E. coli*-derived C was decomposed by other microorganisms, predominantly by fungi, which is supported by the increase in fungal biomass from day 0 to day 7 reported by Zheng et al. (2021). The ratio of ^{13}C-F-GluN/^{13}C-MurA remained more or less constant from day 14 until the end of the experiment (Fig. 2), which further highlighted that a significant percentage of the *E. coli*-derived C was incorporated into fungal necromass grown on the bacterial residues; this material remained in soil until the end of our experiment. Fungal residues have been reported to be more stable than bacterial residues (Schweigert et al., 2015; Six et al., 2006). Additionally, fungal necromass may favour interactions between necromass and minerals or other necromass surfaces. This is likely due to the complex and heterogeneous chemistry of both bacterial and fungal cell walls, containing lipid membranes, peptidoglycan layer as well as layered mannan, β-glucans and chitin (Buckeridge et al., 2020; Dufrêne, 2015), and the hyphal growth of fungi allowing contact to more mineral surfaces. This contributes to adhesion mechanisms that stabilize necromass in soil and may provide an additional essential mechanism for the potential stabilization of ^{13}C derived from bacterial biomass in SOM via transformation into fugal residues. In summary, the combination of the of utilization of ^{13}C-*E. coli* residues by fungi and the higher stability of fungal compared to bacterial residues can result in a high contribution of the labelled *E. coli*-derived C to recalcitrant SOM.

Interestingly, ^{13}C-GalN was formed during the experiment, mainly in the initial phase (first 14 days; Fig. 1C). Although the *E. coli* cells used in the experiment did not contain any GalN as evidenced by analysing a pure culture of the strain for amino sugars (Table. S1), we observed ^{13}C-GalN already at the initial sampling (day 0). This demonstrated that *E. coli* derived C was very quickly incorporated into other microbial

clades in particular fungi. Similarly, the rapid transfer of ^{13}C from *E. coli* into fungal nucleic acids was observed in another soil (Lueders et al., 2006). GalN has been reported to be a component of extracellular polymeric substances (Joergensen, 2018); the further increase may therefore be related to growth and activity of bacteria forming GalN-based extracellular polymeric substance during incubation.

4.3 The metabolic implications on the turnover of bacterial biomass residues

The ^{13}C-amino acids decreased very fast from day 0 to day 7, the decrease slowed down from day 7 to day 30, then they remained relatively stable from day 30 to day 120. In contrast, total amino acids increased significantly during the incubation time (Fig. 3A and 3C). This may indicate that the microbial community was active during the incubation period; the microbes presumably used unlabelled substrates mobilized from SOM for the production of amino acids, and the protein produced must have been stabilized in the soil. The increase in the total amount of hydrolysable amino acids was similar in unamended soil and in soil inoculated with *E. coli* (unlabelled or ^{13}C labelled; Fig. S2), which clearly indicates that SOM mobilization was independent of the addition of bacterial cells. Therefore, the reason for the increase of this parameter cannot be the addition of the bacterial biomass residues. Obviously, the manipulations of the soil necessary to set up the experiment (mixing, moisture adjustment, distribution to microcosms) initiated a strong increase in microbial activity, along with substantial production of amino acids for protein synthesis. The effect was strongest at the beginning of the incubation, although we minimized sample preparation effects on microbial processes in our microcosms by preincubating the soil at 80% of the intended water content and at the incubation temperature.

About 50% of the *E. coli*-derived amino acids were degraded at the end of the experiment. These labelled amino acids may either have been mineralized or converted to other transformation products. These are probably not even necessarily microbial biomass constituents as we did not observe an increase of ^{13}C in fatty acids (see Zheng et al, 2021) or necromass (this study). A potential explanation is that the *E. coli*-derived amino acids may have been utilized by soil nematodes. However, from our results, we cannot provide clear evidence for the fate of the degraded amino acids; we therefore cannot verify any assumptions. Nevertheless, together with the results indicating that the amount of ^{13}C in amino sugars was rather stable during incubation, we can infer that part of the necromass was degraded and mineralized. However, we cannot rule out that necromass was formed with less labelled proteins than the parent biomass. This leads us

393 to the conclusion that microbes utilized amino acids from other (unlabelled) sources,
394 presumably mobilized from SOM, in addition to the (labelled) necromass for their
395 growth (Fig. S3). However, the shift in the pattern of labelled amino sugars to GalN (at
396 the expense of GluN and MurA) indicates that some turnover of the *E. coli*-derived
397 peptidoglycan is taking place and that this material is also used for energy gain.
398 Importantly, we found specific shifts in the ^{13}C-amino acids distribution over time
399 which clearly prove decomposition and synthesis of amino acids (Fig. 3D). In addition,
400 we can use these shifts to get information on shifts in the metabolic pathways of amino
401 acid transformation. The TCA is a central catabolic pathway that provides ATP and
402 reduction equivalents, releases CO_2. However, certain intermediates of this cycle are
403 used for amino acid biosynthesis. In experiments with stable isotope labelled substrates,
404 shifts in the label abundance in different amino acids can thus inform us about how the
405 substrate-derived C is distributed within the central metabolism and the microbial food
406 web. In our study, we observed shifts in ^{13}C-amino acid patterns, which reflect a
407 pronounced shift in the C flow through different branches of the central metabolism, in
408 particular with respect to the biochemical pathways related to the TCA cycle (Fig. 4).
409 Briefly, the first 7 days of incubation can be regarded as a phase of adaptation to the new
410 incubation conditions. Our results showed that the percentage of ^{13}C-glycine within the
411 ^{13}C-amino acids increased in this initial phase (Fig. 3D). Glycine is probably not
412 synthesized from serine, as no label was observed in serine in our study. In addition, we
413 added Gram-negative bacterial biomass residues, which are protein-rich substrates
414 compared to SOM and plant material, at the beginning of the incubation. The lack of
415 carbohydrates for biomass growth (relative to proteins) presumably enhanced the
416 glyoxylate cycle and thus fostered the conversion of glyoxylate directly into glycine
417 (Feisthauer et al., 2008). In the phase of the most active metabolism (day 7 to day 30),
418 we observed that the percentage of ^{13}C-aspartate and ^{13}C-glutamate within ^{13}C-amino
419 acids increased, indicating that the TCA cycle was very active in this phase (Feisthauer
420 et al., 2008). The relatively high activity and growth as well as the related intensive
421 biomass formation require a highly active TCA cycle. At the same time, the demand for
422 biomass building blocks, some of which can be withdrawn from the TCA cycle, is also
423 high. Thus, anaplerotic reactions have to be particularly active in this phase, resulting in
424 high label incorporation into aspartate (Feisthauer et al., 2008; Nowak et al., 2011).
425 Thereafter, from 30 to 120 days, when substrates get exhausted, the metabolism slows
426 down. During this phase, the TCA cycle is less active and the demand for new biomass

components is lower. At this late phase of the incubation, bacterial biomass residues are turned over for preservation of C rather than energy. As a result, the label is preferentially incorporated into amino acids synthesized from pyruvate as a precursor, i.e. alanine and valine, during this phase.

5. Summary and Conclusions

Tracing the ^{13}C derived from labelled *E. coli* biomass residues (representative for Gram-negative bacteria) through amino acids and amino sugars is a prerequisite for understanding the turnover of microbial cell components and can be used to identify the mechanism for stabilization of Gram-negative bacterial biomass-derived C in SOM. In our experiment, we observed that amino sugars are relatively stable biomarkers compared to amino acids. As we expected, the ratio of ^{13}C-F-GluN/ ^{13}C-MurA significantly increased during the first 14 days and then remained relatively stable until the end of the experiment. This suggests that turnover of bacterial biomass residue-derived C is accompanied by a continuous transfer of bacterial-derived C to fungal biomass and its residues. We also observed specific shifts in the ^{13}C-amino acid pattern during turnover of bacterial-derived ^{13}C. These shifts in the label distribution provide a detailed view on shifts in the activity of the TCA cycle and its related metabolism. During the initial incubation period, glyoxylate is converted directly into glycine within the glyoxylate cycle. Then, during the most active metabolism from day 7 to day 30, biomass synthesis requires strong anabolic reactions based on the (unlabelled) SOM resources. In the late phase, the metabolism slows down, as does the TCA cycle. In this phase, bacterial biomass residues are turned over for preservation of C rather than energy at the late phase of the incubation. These findings should be taken into account for the development and refinements of soil C models as they provide theoretical support for a comprehensive understanding of soil C accumulation with microbial mediation.

Our study thus strongly suggests that bacterial biomass residue-derived C is largely transformed to fungal residues. This, however, opens the question of how fungal biomass residues are turned over in soil and how they contribute to the soil C cycle and SOM formation. Additional studies are also needed in order to investigate the effect of exogenous substrates additions on the turnover of both bacterial and fungal biomass residues, and on how we can better disentangle the partially overlapping cycles of bacterial and fungal necromass in soil.

Acknowledgments

This study was financially supported by the National Natural Science Foundation of China (42107324 and 32241037), the National Key Research and Development Program of China (2022YFD1500205), the German Research Foundation (DFG project Mi 598/4), the China Postdoctoral Science Foundation (2021M703396), and the Doctoral Scientific Research Foundation of Liaoning Province of China (2022-BS-024). We greatly acknowledge support with compound-specific analysis of amino acids by Steffen Kümmel, Ursula Günther and Matthias Gehre (UFZ, Department of Isotope Biogeochemistry). General help with laboratory work was provided by Kerstin Ethner and Ines Mäusezahl (UFZ, Department of Environmental Biotechnology). Ines Merbach (UFZ, Department of Community Ecology) provided the soil samples.

References

Amelung, W., 2001. Methods using amino sugars as markers for microbial residues in soil, In: Lal, R., Kimble, J.M., Follett, R.F., Stewart B.A., eds. Assessment Methods for Soil Carbon. CRC/Lewis Publishers, Boca Raton, FL, pp. 233-270.

Buckeridge, K.M., La Rosa, A.F., Mason, K.E., Whitaker, J, McNamara, N.P., Grant, H.K., Ostle, N.J., 2020. Sticky dead microbes: Rapid abiotic retention of microbial necromass in soil. Soil Biology and Biochemistry 149, 107929.

Carter, M.R., 2002. Soil quality for sustainable land management: Organic matter ANS aggregation interactions that maintain soil functions. Agronomy Journal 94, 38-47.

Chapin, F.S., Matson, P. A., Vitousek, P.M., 2011. Principles of terrestrial ecosystem ecology. Springer New York, New York, NY.

Chazdon, R.L., Peres, C.A., Dent, D., Sheil, D., Lugo, A.E., Lamb, D., Stork, N.E., Miller, S.E., 2009. The potential for species conservation in tropical secondary forests. Conservation Biology 23, 1406-1417.

Dufrêne, Y.F., 2015. Sticky microbes: forces in microbial cell adhesion. Trends in Microbiology 23, 376-382.

Engelking, B., Flessa, H., Joergensen, R.G., 2007. Shifts in amino sugar and ergosterol contents after addition of sucrose and cellulose to soil. Soil Biology and Biochemistry 39, 2111-2118.

Farrell, M., Macdonald, L.M., Hill, P.W., Wanniarachchi, S.D., Farrar, J., Bardgett, R.D., Jones, D.L., 2014. Amino acid dynamics across a grassland altitudinal gradient. Soil Biology and Biochemistry 76, 179-182.

Feisthauer, S., Wick, L.Y., Kästner, M., Kaschabek, S.R., Schlömann, M., Richnow, H.H., 2008. Differences of heterotrophic $^{13}CO_2$ assimilation by pseudomonas knackmussii strain B13 and rhodococcus opacus 1CP and potential impact on biomarker stable isotope probing. Environmental Microbiology 10, 1641-1651.

Feofilova, E.P., 2010. The fungal cell wall: modern concepts of its composition and biological function. Microbiology 79, 711-720.

Fernandez, C.W., Langley, J.A., Chapman, S., McCormack, M.L., Koide, R.T., 2016. The decomposition of ectomycorrhizal fungal necromass. Soil Biology and Biochemistry 93, 38-49.

Glaser, B., Gross, S., 2005. Compound-specific $\delta^{13}C$- analysis of individual amino sugars-a tool to quantify timing and amount of soil microbial residue stabilization. Rapid Communications in Mass Spectrometry 19, 1409-1416.

Gunina, A., Dippold, M., Glaser, B., Kuzyakov, Y., 2017. Turnover of microbial groups and cell components in soil: 13C analysis of cellular biomarkers. Biogeosciences 14, 271-283.

Gunina, A., Kuzyakov, Y., 2022. From energy to (soil organic) matter. Global change biology 28, 2169-2182.

Hobara, S., Osono, T., Hirose, D., Noro, K., Hirota, M., Benner, R., 2014. The roles of microorganisms in litter decomposition and soil formation. Biogeochemistry 118, 471-486.

Hu, G., He, H., Zhang, W., Zhao, J., Cui, J., Li, B., Zhang, X., 2016. The transformation and renewal of soil amino acids induced by the availability of extraneous C and N. Soil Biology and Biochemistry 96,

86-96.

Hu, Y., Zheng, Q., Noll, L., Zhang, S., Wanek, W., 2020. Direct measurement of the in situ decomposition of microbial-derived soil organic matter. Soil Biology and Biochemistry 141, 107660.

Joergensen, R.G., 2018. Amino sugars as specific indices for fungal and bacterial residues in soil. Biology and Fertility of Soils 54, 559-568.

Jones, D.L., Kielland, K., 2012. Amino acid, peptide and protein mineralization dynamics in a taiga forest soil. Soil Biology and Biochemistry 55, 60-69.

Kästner, M., Miltner, A., Thiele-Bruhn, S., Liang, C., 2021. Microbial necromass in soils-linking microbes to soil processes and carbon turnover. Frontiers in Environmental Science 9, 756378.

Kindler, R., Miltner, A., Richnow, H., Kastner, M., 2006. Fate of gram-negative bacterial biomass in soil-mineralization and contribution to SOM. Soil Biology and Biochemistry 38, 2860-2870.

Kögel-Knabner, I., 2002. The macromolecular organic composition of plant and microbial residues as inputs to soil organic matter. Soil Biology and Biochemistry 34, 139-162.

Liang, C., Amelung W., Lehmann, J, Kästner, M., 2019. Quantitative assessment of microbial necromass contribution to soil organic matter. Global Change Biology 25, 3578-3590.

Liu, X., Zhou, F., Hu, G., Shao, S., He, H., Zhang, W., Zhang, X., Li, L., 2019. Dynamic contribution of microbial residues to soil organic matter accumulation influenced by maize straw mulching. Geoderma 333, 35-42.

Lueders, T., Kindler, R., Miltner, A., Friedrich, M.W., Kaestner, M., 2006. Bacterial micropredators and fungi distinctively active in a soil food web. Applied and Environmental Microbiology 72, 5342-5348.

Miltner, A., Kopinke, F.D., Selesi, D., Hartmann, A., Kästner, M., 2005a. Non-phototrophic CO_2 fixation by soil microorganisms. Plant and Soil 269, 193-203.

Miltner, A., Richnow, H.H., Kopinke, F.D., Kästner, M., 2005b. Incorporation of carbon originating from CO_2 into different compounds of soil microbial biomass and soil organic matter. Isotopes in Environmental and Health Studies 41, 135-140.

Miltner, A., Kindler, R., Knicker, H., Richnow, H.H., Kästner, M., 2009. Fate of microbial biomass-derived amino acids in soil and their contribution to soil organic matter. Organic Geochemistry 40, 978-985.

Miltner, A., Bombach, P., Schmidt-Brücken, B., Kästner, M., 2012. SOM genesis: microbial biomass as a significant source. Biogeochemistry 111, 41-55.

Nowak, K.M., Miltner, A., Gehre, M., Schaffer, A., Kästner, M., 2011. Formation and fate of bound residues from microbial biomass during 2,4-d degradation in soil. Environmental Science and Technology 45, 999-1006.

Nowak, K.M., Girardi, C., Miltner, A., Gehre, M., Schaffer, A., Kästner, M., 2013. Contribution of microorganisms to non-extractable residue formation during biodegradation of ibuprofen in soil. Science of the Total Environment 445-446, 377-384.

Nowak, K.M., Markus, T., Erika, S., Miltner, A., 2018. Unraveling microbial turnover and non-extractable residues of bromoxynil in soil microcosms with ^{13}C-isotope probing. Environmental Pollution 242, 769-777.

Price, M.N., Zane, G.M., Kuehl, J.V., Melnyk, R.A., Wall, J.D., Deutschbauer, A.M., Arkin, A.P.,

Casadesús, J., 2018. Filling gaps in bacterial amino acid biosynthesis pathways with high-throughput genetics. Plos Genetics 14, e1007147.

R Development Core Team, 2014. R: A Language and Environment for Statistical Computing. R Foundation for Statistical Computing, Vienna, Austria. http://www.R-project.org.

Rillig, M.C., Caldwell, B.A., Wsten, H.A., Sollins, P., 2007. Role of proteins in soil carbon and nitrogen storage: controls on persistence. Biogeochemistry 85, 25-44.

Schweigert, M., Herrmann, S., Miltner, A., Fester, T., Kästner, M., 2015. Fate of ectomycorrhizal fungal biomass in a soil bioreactor system and its contribution to soil organic matter formation. Soil Biology and Biochemistry 88, 120-127.

Shao, S., Zhao, Y., Zhang, W., Hu, G., Xie, H., Yan, J., Han, S., He, H., Zhang, X., 2017. Linkage of microbial residue dynamics with soil organic carbon accumulation during subtropical forest succession. Soil Biology and Biochemistry 114, 114-120.

Silfer, J.A., Engel, M.H., Macko, S.A., Jumeau, E.J., 1991. Stable carbon isotope analysis of amino acid enantiomers by conventional isotope ratio mass spectrometry and combined gas chromatography/isotope ratio mass spectrometry. Analytical Chemistry 63, 370-374.

Six, J., Frey, S.D., Thiet, R.K., Batten, K.M., 2006. Bacterial and Fungal Contributions to Carbon Sequestration in Agroecosystems. Soil Science Society of America Journal 70, 555.

Smith, A.P., Marín-Spiotta, E., Balser, T., 2015. Successional and seasonal variations in soil and litter microbial community structure and function during tropical postagricultural forest regeneration: a multiyear study. Globle Chang Biology 21, 3532-3547.

Stevenson, F.J., 1982. Organic forms of soil nitrogen. In Nitrogen in agricultural soils, Agronomy Monograph no. 22., ASA-CSSA-SSSA, pp. 67-122.

van Groenigen, K.J., Bloem, J., Bååth, E., Boeckx, P., Rousk, J., Bodé, S., Forristal, D., Jones, M.B., 2010. Abundance, production and stabilization of microbial biomass under conventional and reduced tillage. Soil Biology and Biochemistry 42, 48-55.

Yang, Y., Xie, H., Mao, Z., Bao, X., He, H., Zhang, X., Liang, C., 2022. Fungi determine increased soil organic carbon more than bacteria through their necromass inputs in conservation tillage croplands. Soil Biology and Biochemistry 167, 108587.

Zhang, X., Amelung, W., 1996. Gas chromatographic determination of muramic acid, glucosamine, mannosamine, and galactosamine in soils. Soil Biology and Biochemistry 28, 1201-1206.

Zheng, T., Miltner, A., Liang, C., Nowak, K. M., Kästner, M., 2021. Turnover of gram-negative bacterial biomass-derived carbon through the microbial food web of an agricultural soil. Soil Biology and Biochemistry 152, 108070.

613 **Figure Legends**

614

615 **Fig. 1.** Absolute abundance of total amino sugars (A) and percentage of total amino
616 sugars (B), as well as absolute abundances of ^{13}C-amino sugars (C) and percentage of
617 ^{13}C-amino sugar (D) during incubation. GluN, glucosamine; MurA, muramic acid; GalN,
618 galactosamine. Error bars represent standard errors. Different letters denote significant
619 differences between sampling times ($P < 0.05$).

620

621 **Fig. 2.** Ratio ^{13}C-F-GluN to ^{13}C-MurA during incubation. GluN, glucosamine; MurA,
622 muramic acid. Error bars represent standard errors. Different letters denote significant
623 differences between incubation times ($P < 0.05$).

624

625 **Fig. 3.** Absolute abundance of total amino acids (A) and percentage of total amino acids
626 (B), as well as absolute abundance of ^{13}C-amino acids (C) and percentage of ^{13}C-amino
627 acids (D) during incubation time. Error bars represent standard errors. Different letters
628 denote significant differences between incubation time ($P < 0.05$).

629

630 **Fig. 4.** Simplified conceptual model indicating the shifts of the central metabolism as
631 indicated by shifts in ^{13}C-amino acid distribution over incubation time. Orange
632 background indicates increased ^{13}C-amino acid percentage; blue background indicates
633 decreased ^{13}C-amino acid percentage. The green lines indicated the potentially dominant
634 pathway in each phase according to the observed shifts in ^{13}C-amino acid abundances.

635

636

637

638

639

640

641

642

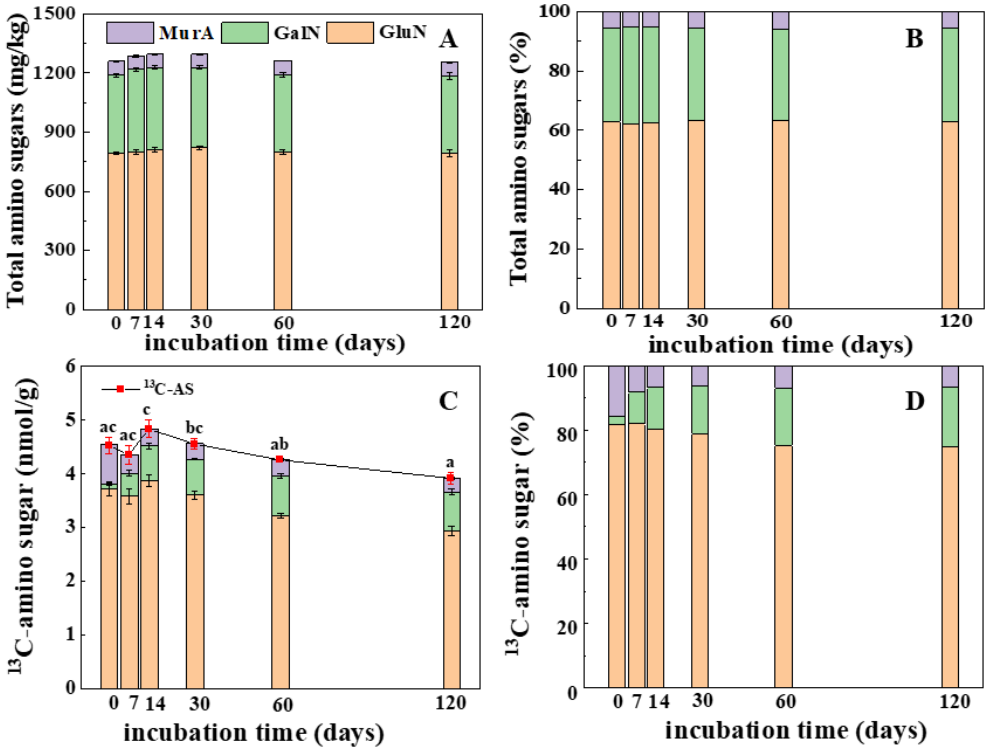

643

644 Fig.1. Absolute abundance of total amino sugars (A) and percentage of total amino
645 sugars (B), as well as absolute abundances of ^{13}C-amino sugars (C) and percentage of
646 ^{13}C-amino sugar (D) during incubation. GluN, glucosamine; MurA, muramic acid; GalN,
647 galactosamine. Error bars represent standard errors. Different letters denote significant
648 differences between sampling times ($P < 0.05$).

649

650

651

652

653

654

655

656

657

658

659

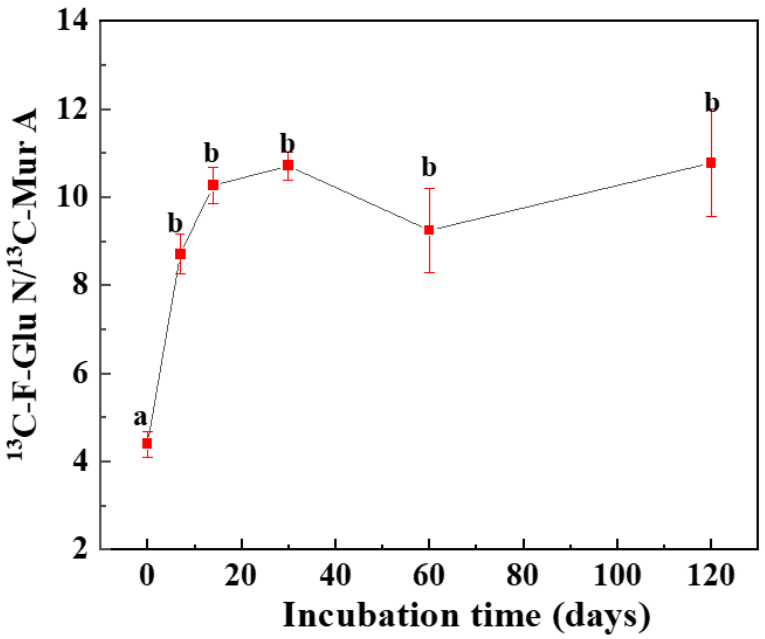

Fig.2. Ratio ^{13}C-F-GluN to ^{13}C-MurA during incubation. GluN, glucosamine; MurA, muramic acid. Error bars represent standard errors. Different letters denote significant differences between incubation times ($P < 0.05$).

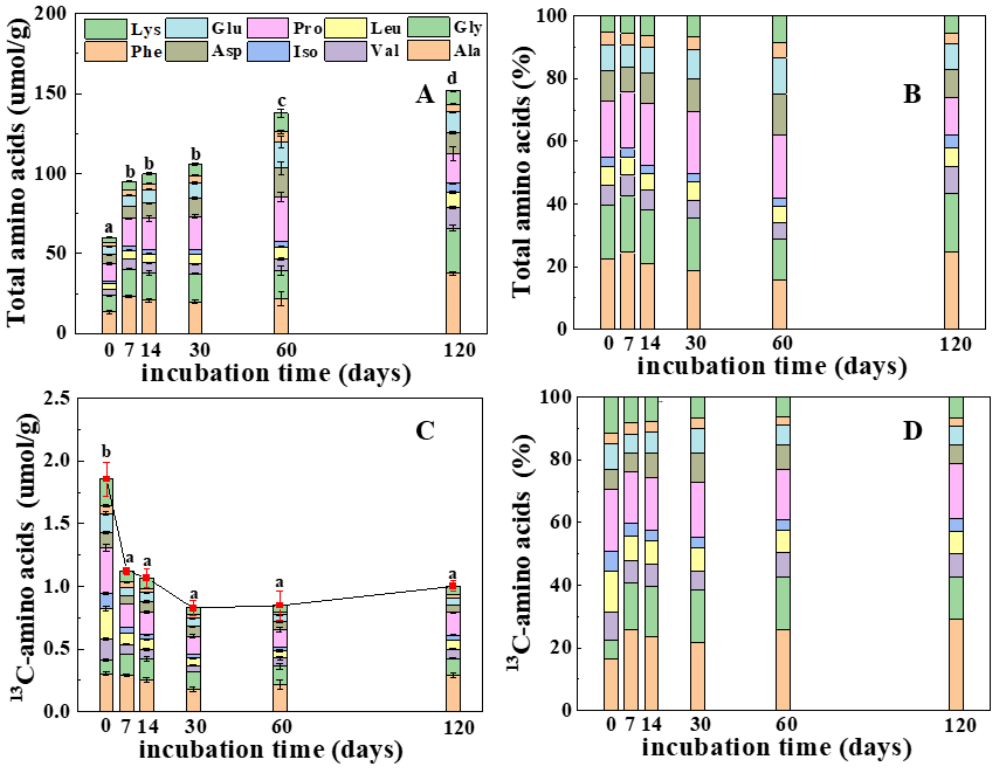

Fig.3. Absolute abundance of total amino acids (A) and percentage of total amino acids (B), as well as absolute abundance of ^{13}C-amino acids (C) and percentage of ^{13}C-amino acids (D) during incubation time [Lys (Lysin), Phe (Phenylalanine), Glu (Glutamat), Asp (Aspartat), Pro (Proline), Iso (Isoieucine), Leu (Leucine), Val (Valine), Gly (Glycine), Ala (Alanine)]. Error bars represent standard errors. Different letters denote significant differences between incubation time ($P < 0.05$).

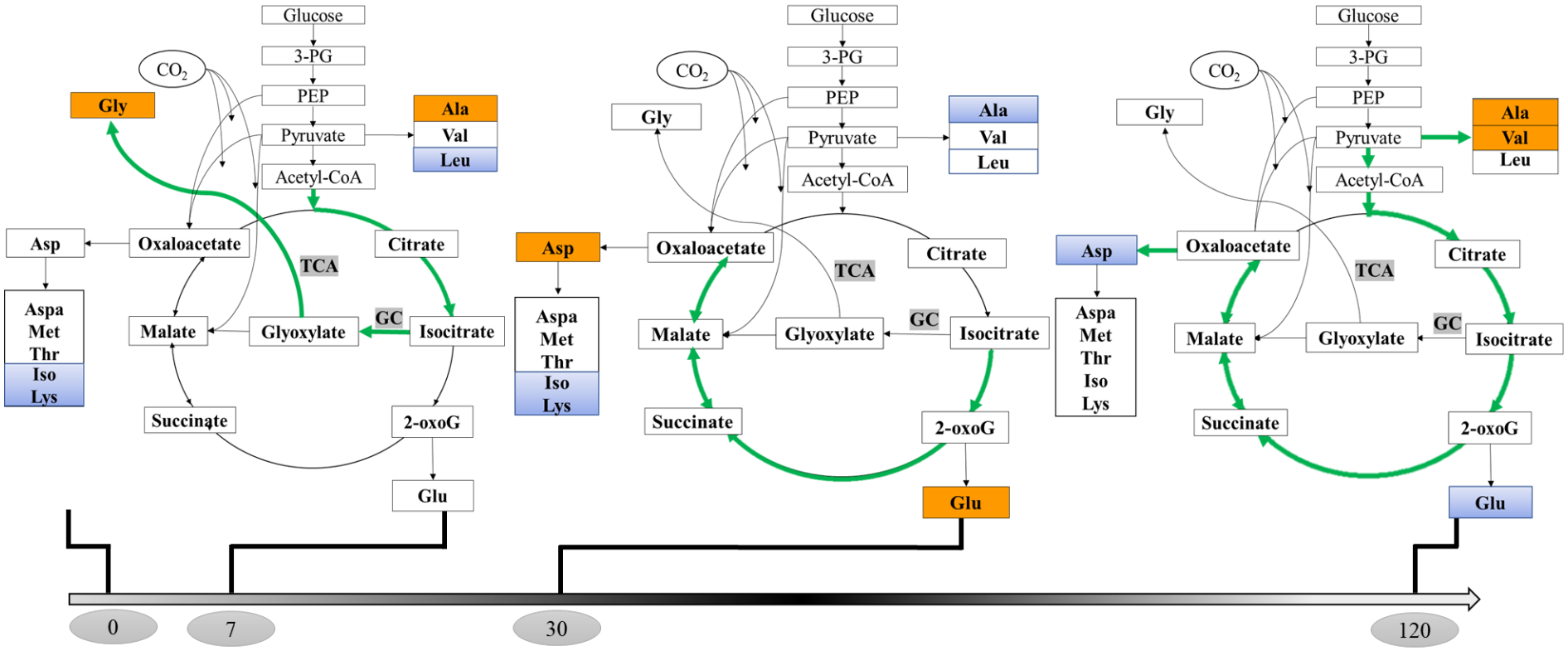

Fig. 4. Simplified conceptual model indicating the shifts of the central metabolism as indicated by shifts in ^{13}C-amino acid distribution over incubation time. Orange background indicates increased ^{13}C-amino acid percentage; blue background indicates decreased ^{13}C-amino acid percentage [Lys (Lysin), Phe (Phenylalanine), Glu (Glutamat), Asp (Aspartat), Pro (Proline), Iso (Isoieucine), Leu (Leucine), Val (Valine), Gly (Glycine), Ala (Alanine), Aspa (Asparagine), Met (Methionine), Thr (Threonine)]. TCA: tricarboxylic acid cycle, GC: glyoxylate cycle. The green line indicated the potentially dominant pathway in each phase according to the observed shifts in ^{13}C-amino acid abundances.